



# Growth of controlled thickness graphene by ion implantation for field-effect transistor

Gang Wang<sup>a,b</sup>, Guqiao Ding<sup>b</sup>, Yun Zhu<sup>b</sup>, Da Chen<sup>a</sup>, Lin Ye<sup>a</sup>, Li Zheng<sup>b</sup>, Miao Zhang<sup>b</sup>, Zengfeng Di<sup>b</sup>, Su Liu<sup>a,\*</sup>

<sup>a</sup> School of Physical Science and Technology, Lanzhou University, 222, Tianshui, Lanzhou 730000, China

<sup>b</sup> State Key Laboratory of Functional Materials for Informatics, Institute of Microsystem and Information Technology, Chinese Academy of Sciences, Shanghai 200050, China

## ARTICLE INFO

### Article history:

Received 11 May 2013

Accepted 2 June 2013

Available online 7 June 2013

### Keywords:

Graphene

Raman

Controlled thickness

Electrical properties

Semiconductors

## ABSTRACT

In contrast to the commonly employed chemical vapor deposition growth on nickel bulk that leads to multilayer graphene formation by carbon segregation, we present an approach to synthesize high quality graphene on Ni through carbon ion implantation and post annealing. Through tuning the dose of carbon ions with the aid of ion beam technology, followed by high-temperature annealing and fast cooling down, graphene layer with the desired thickness has been achieved. Raman, HRTEM and optical transmittance spectra are used to determine both the quality and thickness of the graphene film. We have fabricated and characterized the field effect transistors to determine the electrical properties of the synthesized graphene film. Furthermore, our technique can utilize standard equipments available in semiconductors technology.

© 2013 Elsevier B.V. All rights reserved.

## 1. Introduction

Graphene is a one-atom-thick carbon material that has attracted great scientific and technological interest due to its intriguing physical properties and enormous potential for various applications [1]. There are several approaches proposed to synthesize graphene, such as micromechanical exfoliation [2], epitaxial growth on silicon carbide [3], and reduction of graphite oxide [4,5]. At present, simple thermal decomposition of hydrocarbons on the surface, or surface segregation of carbon upon cooling from a metastable carbon-metal solid solution, is becoming a method of choice to prepare large-area graphene film on various transition metal substrates, such as copper (Cu) and nickel (Ni). Because of a low carbon solubility in Cu, graphene film grows on Cu catalyst almost exclusively as a single layer [6]. In the case of Ni, where carbon has a significant temperature-dependent solubility, various graphene layers can be produced with different the reaction time and the cooling rate, allowing some control over the number of produced graphene layers [7]. However, it seems difficult to precisely control the number of graphene layers. Many experimental results suggest that controlling the cooling rate during the chemical vapor deposition (CVD) process may not be an appropriate parameter to control the thickness of graphene film,

namely because the deposition and segregation process may occur simultaneously during graphene growth [8,9]. In this work, we propose a way that may overcome this bottleneck by ion implantation of carbon in Ni foils to synthesis of high-quality graphene with controllable thickness. Ion implantation technique can accurately control the carbon content and the uniformity of the in-plane carbon concentration in the Ni foils. Through tuning the implantation dose of carbon ions, graphene layer with the desired thickness has been achieved. Electrical properties of FET analysis reveal that graphene has high quality.

## 2. Experimental

Our fabrication procedure starts with preliminary treatment of the  $1 \times 1 \text{ cm}^2$  Ni foils (25  $\mu\text{m}$ , Alfa Aesar, item No. 1204). The synthesis was carried out in a horizontal tube furnace with a quartz processing tube inside (50 mm inner diameter). The quartz tube was evacuated to approximately  $10^{-5}$  mbar and then filled with 200 standard cubic cm per min (sccm) Argon (Ar, 99.9999% purity) and 50 sccm Hydrogen ( $\text{H}_2$ , 99.9999% purity). After heating to 1000 °C for 1 h at ambient pressure, 10–20  $\mu\text{m}$  crystal grains with atomically flat surface were achieved on Ni foils. And then 30 keV  $\text{C}^+$  ions were implanted into annealed Ni foils with the doses of  $4 \times 10^{15}$  atoms/ $\text{cm}^2$  and  $8 \times 10^{15}$  atoms/ $\text{cm}^2$ , which correspond to monolayer graphene and bilayer graphene, respectively. The projected range

\* Corresponding author. Tel.: +86 931 8912617; fax: +86 931 8913554.  
E-mail address: [liusu\\_lzu@126.com](mailto:liusu_lzu@126.com) (S. Liu).

of the implanted ions was estimated to be 30 nm for 30 keV based on the SRIM-2000 code. The implanted substrates were thermally treated at 980 °C for 30 min under ambient pressure. Graphene layer was precipitated on Ni foils after rapidly cooled to room temperature at a rate of  $\sim 200$  °C min<sup>-1</sup>. Fig. 1 schematically shows the procedure followed in this work. Graphene was characterized using Raman spectroscopy (HORIBA Jobin Yvon HR800), transmission electron microscopy (TEM, FET-Tecni G2F20 S-7WIN) and optical transmittance spectra (UV solution U-4100).

### 3. Results and discussion

#### 3.1. Raman analysis

Raman spectroscopy was used to determine both the quality and thickness of the graphene film with different implantation doses. Fig. 2(a) depicts the representative Raman spectrum of the as-deposited graphene showing G band around at  $\sim 1580$  cm<sup>-1</sup>. The 2D band is around at  $\sim 2700$  cm<sup>-1</sup>, which is the main hallmark of

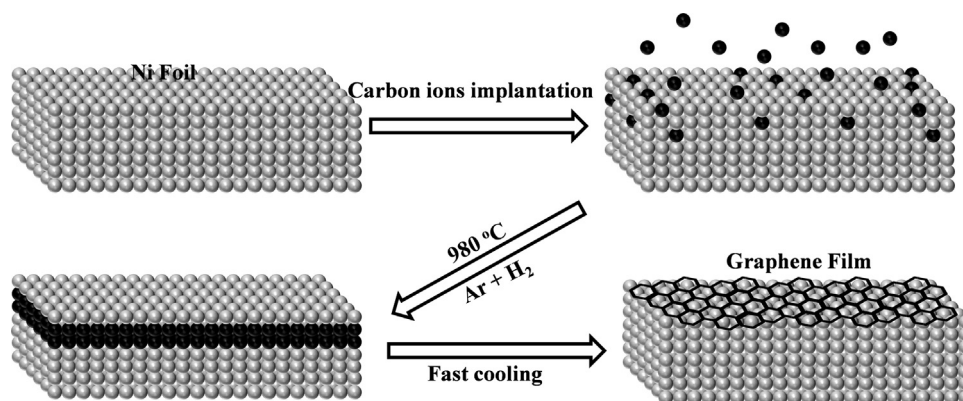


Fig. 1. Schematic illustration of the procedure used in this work.

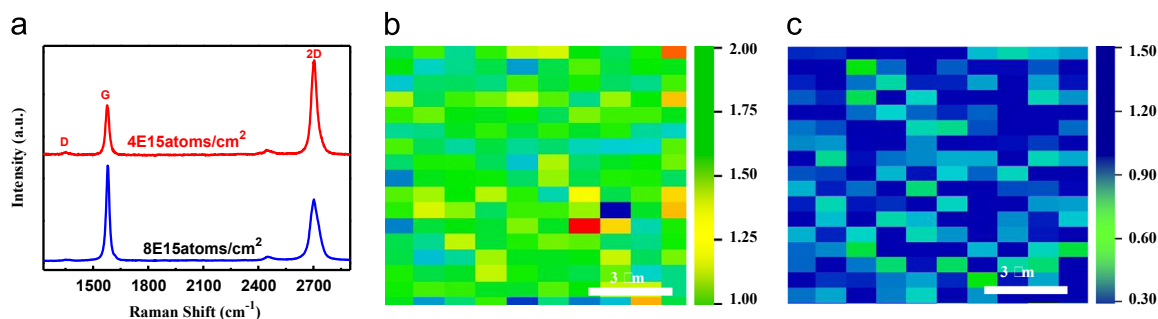


Fig. 2. (a) Raman spectrum of graphene film grown on Ni foils implanted with the doses of  $4 \times 10^{15}$  atoms/cm<sup>2</sup> and  $8 \times 10^{15}$  atoms/cm<sup>2</sup>, respectively.  $I_{2D}/I_G$  band ratio Raman mapping measurements of graphene films grown under different dose of carbon ions. (b)  $4 \times 10^{15}$  atoms/cm<sup>2</sup> and (c)  $8 \times 10^{15}$  atoms/cm<sup>2</sup>.

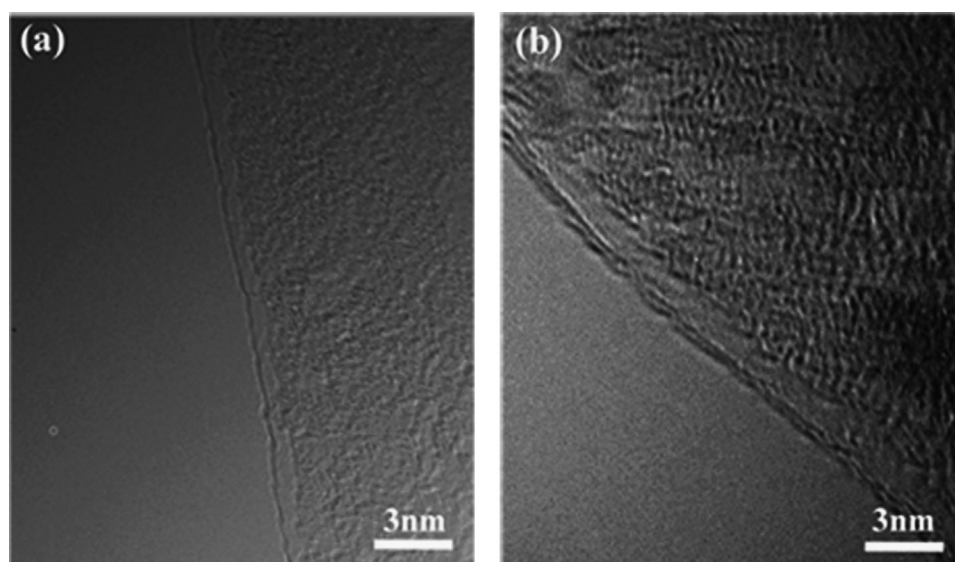


Fig. 3. (a) HRTEM image of monolayer graphene edges that show one carbon layer. (b) HRTEM image of bilayer graphene edges that show two carbon layers.

graphene and sensitive to the number of layers and the quality of graphene. The relatively low intensity of D band suggests that synthesized graphene films is in high quality comparable to that of CVD grapheme [10]. When the dose of carbon ions is  $4 \times 10^{15}$  atoms/cm<sup>2</sup>, only monolayer graphene film grows with an  $I_{2D}/I_G$  ratio more than 1.5. The symmetric 2D band with a full width at half maximum (FWHM) of  $\sim 30$  cm<sup>-1</sup> can be well fitted by a single Lorentzian curve. With further increasing the dose of carbon ions to  $8 \times 10^{15}$  atoms/cm<sup>2</sup>, bilayer graphene comes into being on Ni surface as the average  $I_{2D}/I_G$  decreases to  $\sim 0.5$ . The symmetric 2D band with a FWHM of  $\sim 45$  cm<sup>-1</sup> can be well fitted by a four Lorentzian curves [11,12]. Statistically, Raman mapping at the  $12 \times 12 \mu\text{m}^2$  scale confirms the thickness and uniformity of graphene films. In a typical monolayer graphene film (as shown in Fig. 2(b)), more than 90% of the graphene area has an  $I_{2D}/I_G$  ratio  $> 1.25$ . In Fig. 2(c), no monolayer Raman signature ( $I_{2D}/I_G > 1.25$ ) is observed at any pixel on the map and  $\sim 85\%$  of the film has an  $I_{2D}/I_G$  ratio of 0.3–0.6, suggesting uniform bilayer graphene.

### 3.2. HRTEM analysis

Graphene films were transferred from the Ni foils onto TEM grids by a PMMA-assisted wet-transfer method in order to directly evaluate the thickness of the graphene films. Fig. 3(a) and (b) is the typical high resolution transmission electron microscopy (HRTEM) images of graphene edges. HRTEM images of monolayer and bilayer

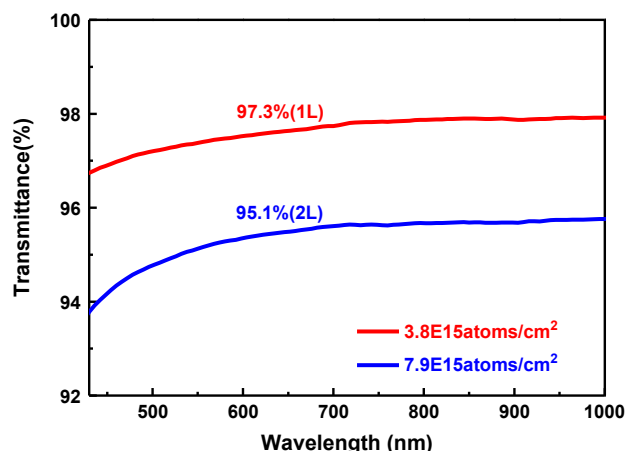


Fig. 4. Transmittance of monolayer and bilayer graphene films obtained with visible-absorption spectroscopy on quartz substrates. The transmittance of graphene was measured at 550 nm.

graphene edges show one and two carbon layers for  $4 \times 10^{15}$  atoms/cm<sup>2</sup> and  $8 \times 10^{15}$  atoms/cm<sup>2</sup> +C implanted in Ni foils, respectively.

### 3.3. Transmittance properties analysis

To further evaluate the controllable thickness of graphene films, the transmittance at 550 nm is obtained from the graphene film transferred onto glass slides and the results are presented in Fig. 4. The optical transmittance diminishes gradually as the dose of carbon ions is varied from  $4 \times 10^{15}$  atoms/cm<sup>2</sup> to  $8 \times 10^{15}$  atoms/cm<sup>2</sup> +C, supplying evidence that the graphene film become thicker. For the graphene film obtained from the Ni foil implanted with  $4 \times 10^{15}$  atoms/cm<sup>2</sup>, a high transparency of 97.51% is observed. Considering an absorbance of  $\sim 2.3\%$  for an individual graphene layer [13], the graphene film can be inferred to have only one layer. When the dose of carbon ions is changed to  $8 \times 10^{15}$  atoms/cm<sup>2</sup> +C, the transmittance drops to 96.20%, and the graphene film is composed of two layers, in good agreement with the predicted and the reported [14].

### 3.4. Electrical properties analysis

To determine the transport properties of the synthesized graphene films, back-gated graphene field effect transistors (GFETs) were fabricated on 300 nm SiO<sub>2</sub>/Si substrates, as shown in the inset of Fig. 5. Fig. 5(a) and (b) shows the highly reproducible transfer characteristics ( $I_{DS}-V_G$ ) of the GFETs measured at room temperature under ambient conditions for monolayer and bilayer graphene. The typical  $I_{DS}-V_G$  curve measured at a  $V_{DS}$  of 100 mV shows that the gate can cause either hole or electron conduction. The Dirac point of the GFETs shifts slightly to a positive gate at  $V_G \sim 30$  V, demonstrating light p-type hole doping performance. According to the two slopes of the linear regions on both sides of the “U” shaped curve, the hole mobility is  $\mu_h \sim 950$  cm<sup>2</sup> V<sup>-1</sup> s<sup>-1</sup> and the electron mobility is  $\mu_e \sim 900$  cm<sup>2</sup> V<sup>-1</sup> s<sup>-1</sup> for monolayer. Similarly, the hole mobility is  $\mu_h \sim 880$  cm<sup>2</sup> V<sup>-1</sup> s<sup>-1</sup> and the electron mobility is  $\mu_e \sim 840$  cm<sup>2</sup> V<sup>-1</sup> s<sup>-1</sup> for bilayer. Both of which are comparable to values reported recently from transferred CVD grapheme [15]. The electrical transport data also reveal that the graphene synthesis by ion implantation has good quality, and can be further improved by refining the deposition process.

## 4. Conclusion

In summary, we describe a straightforward technique for graphene films synthesis and graphene thickness control with the aid of ion implantation. The advantages of ion implantation

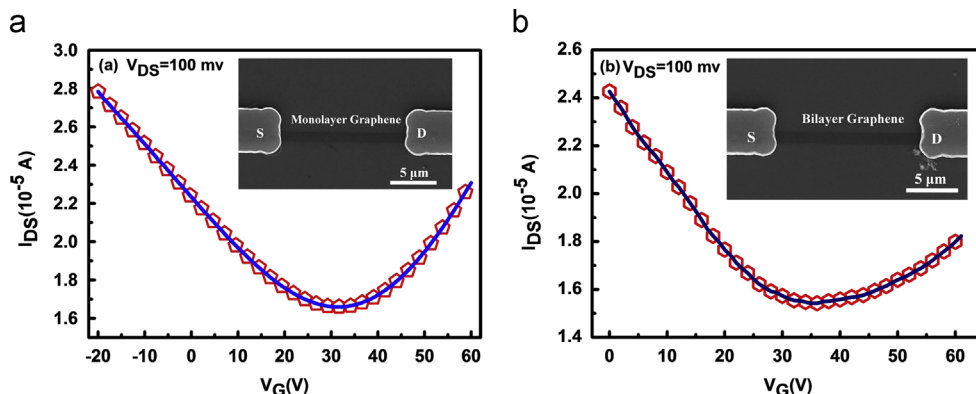


Fig. 5. (a)  $I_{DS}-V_G$  curve of monolayer graphene transistors at  $V_{DS} = 100$  mV. (b)  $I_{DS}-V_G$  curve of bilayer graphene transistors at  $V_{DS} = 100$  mV. (The insert shows the SEM image of a back-gated GFET.)

synthesis method are suitable for variety of metal substrates, since it does not require thermal decomposition of hydrocarbons on the surface or solvation of carbon into the substrate. Raman, HRTEM, optical transmittance spectra and electrical properties characterizations confirm that the graphene films grown by ion implantation have good crystallinity and thickness controllability. Our technique can utilize standard equipments available in semiconductor technology which is maturity and scalable.

### Acknowledgements

We thank the supports from the National Natural Science Foundation of China under Grant No. 61176001, 51222211, 61006088, the National Basic Research Program of China (973 Program) under Grant No. 2010CB832906, the Pujiang Talent Project of Shanghai under Grant No. 11PJ1411700, and the One Hundred Talent project from Chinese Academy of Sciences.

### References

- [1] Yang Z, Gao RG, Hu NT, Chai J, Cheng YW, Zhang LY, et al. *Nano-Micro Lett* 2012;4:1–9.
- [2] Novoselov KS, Geim AK, Morozov SV, Jiang D, Zhang Y, Dubonos SV. *Science* 2004;306:666–9.
- [3] Berger C, Song Z, Li X, Wu S, Brown N, Naud C, et al. *Science* 2006;312:1191–6.
- [4] Park S, Ruoff R. *Nat Nanotechnol* 2009;4:217–24.
- [5] Yin KB, Li HT, Xia YD, Bi HC, Sun J, Liu ZG, et al. *Nano-Micro Lett* 2011;3:51–5.
- [6] Li X, Cai W, An J, Kim S, Nah J, Yang D, et al. *Science* 2009;324:1312–4.
- [7] Yu Q, Lian J, Siriponglert S, Li H, Chen Y, Pei S. *Appl Phys Lett* 2008;93:113103.
- [8] Addou R, Dahal A, Sutter P, Batzill M. *Appl Phys Lett* 2012;100:021601.
- [9] Chae S, Guenes F, Kim K, Kim S, Han G, Shi H, et al. *Adv Mater* 2009;21:2328–33.
- [10] Gong Y, Zhang X, Liu G, Wu L, Geng X, Long M, et al. *Adv Funct Mater* 2012;22:3153–9.
- [11] Park J, Mitchel W, Grazulis L, Smith H, Eyink K, Boeckl J, et al. *Adv Mater* 2010;22:4140–5.
- [12] Peng Z, Yan Z, Sun Z, Tour J. *ACS Nano* 2011;5:8241–7.
- [13] Nair RR, Blake P, Grigorenko AN, Novoselov KS, Booth TJ, Stauber T, et al. *Science* 2008;320:1308–1308.
- [14] Pimenta M, Dresselhaus G, Dresselhaus M, Cancado L, Jorio A, Saito R. *Phys Chem Chem Phys* 2007;9:1276.
- [15] Bae S, Kim H, Lee Y, Xu X, Park J, Zheng Y, et al. *Nat Nanotechnol* 2010;5:574–8.